Received: 30 September 2020 | Revised: 25 January 2021 | Accepted: 27 January 2021

DOI: 10.1002/dta.3007

RESEARCH ARTICLE

WILEY

Metabolic profiling of deschloro-*N*-ethyl-ketamine and identification of new target metabolites in urine and hair using human liver microsomes and high-resolution accurate mass spectrometry

Islam Amine Larabi[1] | Fanny Zerizer[1] | Alice Ameline[2] | Isabelle Etting[1] | Delphine Joseph[3] | Pascal Kintz[2,4] | Jean Claude Alvarez[1]

[1]Department of Pharmacology and Toxicology, Paris-Saclay University (Versailles Saint-Quentin-En-Yvelines University), Garches, France

[2]X-Pertise Consulting, Mittelhausbergen, France

[3]CNRS, BioCIS, Université Paris-Saclay, Châtenay-Malabry, France

[4]CHU de Strasbourg, Institut de Médecine Légale, Strasbourg, France

Correspondence
Prof. Jean Claude Alvarez and Dr. Islam Amine Larabi, Laboratoire de Pharmacologie-Toxicologie, Université de Versailles Saint-Quentin en Yvelines, Inserm U-1173. Hôpital Raymond Poincaré, AP-HP, 104, Boulevard R. Poincaré, 92380 Garches, France.
Email: jean-claude.alvarez@aphp.fr; islamamine.larabi@aphp.fr

Abstract

The aim of this study was to identify new markers of deschloro-*N*-ethyl-ketamine (O-PCE), a ketamine analogue that has been involved in acute intoxications with severe outcomes including death and whose metabolism has never been studied before. In vitro study after 2-h incubation with pooled human liver microsomes (HLMs) cross-checked by the analysis of urine and hair from a 43-year-old O-PCE user (male) were performed by liquid chromatography–high resolution mass spectrometry (LC-HRMS). Acquired data were processed by the Compound Discoverer® software, and a full metabolic profile of O-PCE was proposed. In total, 15 metabolites were identified, 10 were detected in vitro (HLMs) and confirmed in vivo (urine and/or hair), two were present only in HLMs, and the remaining three metabolites were identified only in biological specimens. While O-PCE was no longer detected in urine, nine metabolites were identified allowing to increase its detection window. In descending order of metabolites abundance, we suggest using 2-en-PCA-*N*-Glu (34%, first), M3 (16%, second), O-PCA-*N*-Glu (15.4%, third), OH-O-PCE (15%, fourth) and OH-PCE (11.9%, fifth) as target metabolites to increase the detection window of O-PCE in urine.

In hair, nine metabolites were identified. OH-PCA was the major compound (78%) with a relevant metabolite to parent drug ratio (=6) showing its good integration into hair and making it the best marker for long-term monitoring of O-PCE exposure.

KEYWORDS
deschloro-*N*-ethyl-ketamine, hair, high-resolution mass spectrometry, human liver microsomes, new psychoactive substances

1 | INTRODUCTION

Hallucinogens are a diverse group of naturally occurring or synthetic drugs that produce altered perception of reality known as 'Synaesthesia' observed with *classic hallucinogens* (e.g., LSD, dimethyltryptamine and 5-MeO-DMT), also referred to as 'psychedelics', or a feeling of detachment and dissociation from the self and the environment encountered with *dissociative anaesthetics* (e.g., ketamine, phencyclidine and methoxetamine). Classic hallucinogens act as serotonin receptor agonists while dissociative anaesthetics possess both stimulant and dissociative properties by inhibiting the reuptake of dopamine, norepinephrine and serotonin, and modulating effects at

the *N*-methyl-D-aspartate (NMDA) receptor in the brain.[1] New psychoactive substances (NPS) are a range of drugs that mimic established illicit drugs of abuse, such as cannabis, MDMA and ketamine. In 2017, hallucinogens accounted for 18% of the 492 NPS reported to the UNODC (United Nations Office On Drugs and Crime).[1]

In the last decade, recreational use of ketamine has gained popularity, especially in Asia (India, China), and part of Europe (Netherlands, Belgium, France). Among the 47 countries reporting ketamine seizures to UNODC over the period 2001–2017, 21 were in Europe and 16 in Asia.[1,2] By slight chemical modification on ketamine scaffold, a wide variety of compounds with similar or even more pronounced effects have been clandestinely synthesized. Among these, deschloro-*N*-ethyl-ketamine, known to as 'eticyclidone', '2-oxo-PCE' or 'O-PCE' has reappeared in 2016 for the first time in France, after early studies on its anaesthetic effect conducted by Stevens in 1966 to overcome phencyclidine (PCP) adverse effects.[3,4] O-PCE is an aryl-amino-cyclohexan-2-one derivative that share with ketamine and methoxetamine (MXE) the core structure of 2-phenyl-2-aminocyclohexanone. Ketamine has a chlorine atom at the 2-position of the phenyl ring and a methyl group on the amine function; O-PCE differs by the presence of an ethyl substituent instead of the methyl group on the amine group and of an unsubstituted phenyl ring; and MXE has a similar structure than O-PCE with an additional methoxy group at the 3-position of the phenyl ring (Figure 1).[5]

Although extensive pharmacological and toxicological data are available for ketamine, and to some extent for MXE, only few overdose cases with analytically confirmed acute O-PCE toxicity have been reported recently.[6,7] The main clinical symptoms associated with O-PCE use included impaired consciousness (84%), confusion (60%), abnormal behaviour (44%), hypertension (80%), tachycardia (40%) and convulsions (16%). The toxicity of O-PCE was reported to be more severe than ketamine as it seemed more potent at low dose.[6] Moreover, O-PCE can be used alone, or in mixture with ketamine or other drugs of abuse (methamphetamine, MDMA, pentylone), which could lead to more toxicity as reported by Cheng et al.[5] In this study, O-PCE and its metabolite deschloro-norketamine were detected in blood in four driving under the influence (DUID) cases in the range of 80–310 and 40–90 ng/ml, respectively.[5] Knowledge about the metabolic pathways allows method development targeting the most relevant markers of drug intake, including parent drug and/or metabolites. It also explores drug–drug interaction, which may explain some of the reported effects. For ethical reasons, studies in humans are not possible to perform. Hence, in vivo animal experiments or in vitro approaches are employed as an alternative.[8] While studies using animals require specific facilities, in vitro metabolism models seem more convenient in most forensic laboratories equipped with mass spectrometry and/or nuclear magnetic resonance (NMR)-based instruments. Human liver microsomes (HLMs) are among the most well established and frequently used in vitro tools in forensic and clinical pharmacology and toxicology.[9–15] This model allows to investigate the formation of phase I and some phase II metabolites (e.g., glucuronides), and to elucidate their chemical structure, and the kinetic of formation, mostly by using high-resolution mass spectrometry.[16]

To our knowledge, there are currently no data regarding O-PCE metabolic pathways; thus, the aim of this study was to elucidate its metabolic profile using HLMs and to identify new target metabolites that can be used as markers for its detection in humans. The proposed metabolic scheme was validated by analysing urine and hair specimens from an O-PCE user by high-resolution accurate mass spectrometry (HRMS).

2 | EXPERIMENTAL PROCEDURES

2.1 | Chemicals and reagents

Alamethicin (*Trichoderma viride*), tris hydrochloride (HCl), magnesium chloride anhydrous, uridine 5′-diphosphoglucuronic acid tris (UDPGA), glucose-6-phosphate dehydrogenase (G6PDH), D-glucose 6-phosphate (G6P), reduced form of nicotinic acid adenine

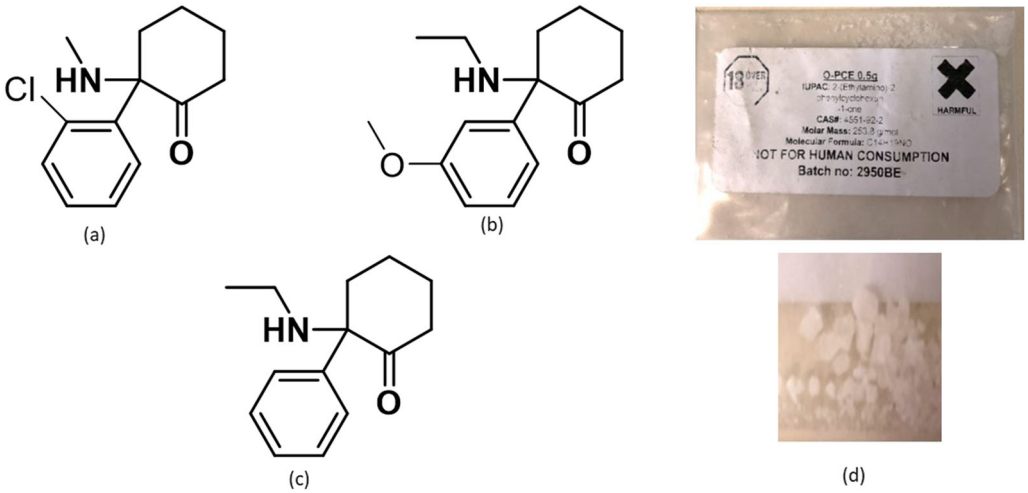

FIGURE 1 Structure of ketamine (a) and its derivatives methoxetamine (MXE) (b) and O-PCE (c) as a crystalline solid (d) labelled 'not for human consumption' and used in the present study

dinucleotide phosphate (NADPH, 98%) were provided by Sigma-Aldrich (France).

A pool of HLMs at a concentration of 25 mg of microsomal protein per millilitre obtained from 17 donors (seven females and 10 males) aged 31–78 years was purchased from Biopredic (La Bretèche, Saint Grégoire, France) and stored at −80°C until use.

Acetonitrile (ACN), chloroform, isopropranol, ethyl acetate, formic acid, hexane and methanol (MeOH) were purchased from Sigma Aldrich (Paris, France) in mass spectrometry (MS) or high-performance liquid chromatography (HPLC) grades; sodium carbonate and hydrogen carbonate were purchased from Prolabo (Paris, France). Ultrapure water (18 MΩ) was obtained by ultrafiltration with a Q-Pod (Millipore Corp., Molsheim, France). Formate buffer containing 2 mM ammonium formate in 0.1% formic acid was prepared in ultra-pure water and stored at +4°C away from light for a maximum of 1 week. Methanolic solutions of O-PCE were prepared from a crystalline solid (purity: 99%) at 1 and 0.1 mg/ml, and stored at −20°C.

2.2 | NMR analysis

The purity of O-PCE purchased from the Internet by a drug user and recovered during harm reduction session was assessed by NMR analysis, according to a previously published procedure.[17] Briefly, an aliquot of 10–30 mg of material is dissolved in deuterated methanol and analysed. Proton 1H, carbon 13C and DEPT carbon 13 NMR were performed. Two-dimensional (2D) NMR was also performed: correlated spectroscopy (COSY), heteronuclear single quantum correlation (HSQC) and heteronuclear multiple-bond correlation (HMBC). NMR spectra were recorded with Brüker Avance spectrometers operating at 300 MHz and equipped with BBFO probe.

2.3 | In vitro incubation with HLMs

The procedure is derived from previous publications[13,15]; 100 µl of HLMs solution (25 mg/L) were activated by 250 µl of alamethicin (50 µM) on crushed ice after adding 150 µl of Tris-HCl (100 mM)-$MgCl_2$ (10 mM) buffer solution (pH 7.4); 50 µl of this mixture were added to a vial containing 50 µl of O-PCE solution (394 µM) previously dried under a gentle stream of nitrogen; 50 µl of a cofactor solution (5 mM UDPGA, 3.2 mM NADPH, 8.5 mM G6P and 0.5 U/ml G6PD) prepared in the same buffer (Tris-HCl-$MgCl_2$) were added. The enzymatic reaction was monitored for 2 h at 37°C and was quenched with 200 µl of MeOH. Samples were centrifuged at 4°C for 14 min at 14,000 rpm, and 10 µl of the supernatant were injected onto the chromatographic system.

Two zero points consisting respectively of HLMs incubates without the addition of substrate (O-PCE) (blank HLMs-1) to subtract background signal related to the matrix or without adding cofactors (blank HLMs-2) to prevent misinterpretation of not metabolically formed metabolites during drying and/or incubation process were analysed simultaneously.

2.4 | LC-HRMS analysis

2.4.1 | Sample preparation

Two hundred microlitres of nonhydrolysed urine or 20 mg of decontaminated hair (using two bath of dichloromethane) underwent liquid–liquid extraction using 4 ml of hexane/ethyl acetate (1/1, v/v). After agitation for 10 min and centrifugation for 10 min at 14,000 rpm, the organic phase was recovered, and the aqueous phase underwent a second extraction by 4 ml of chloroform/isopropanol (80/20, v/v). The two organic phases were merged and evaporated to dryness. The residue was reconstituted in 80 µl of mobile phase, and 10 µl were injected onto the chromatographic system.

2.4.2 | Instrument conditions

The LC-HRMS procedure has already been published.[18] Briefly, chromatographic separation was performed on an Ultimate 3000 pump (Thermo Fisher, Les Ulis, France) using a phenyl-hexyl column (PH, 100 × 2.1 mm i.d., 2.6-µm particle size, Thermo, Waltham, USA) maintained at 40°C. The flow rate was set at 500 µl/min. Elution was achieved in gradient mode using a mixture of water/ammonium formate 2 mM/0.1% formic acid (solvent A) and ACN/MeOH (50:50, v/v)/1% water/0.1% formic acid (solvent B). The total run was of 20 min with a gradient of B (1%–99%) of 17.5 min.

Compounds were detected using an Orbitrap accurate mass spectrometer (Q-Exactive, Thermo, Waltham, USA) equipped with a heated electrospray ionization (HESI) probe operating in positive-ion mode. Data were acquired in data-dependent acquisition (DDA) mode. MS cycles were composed of one full MS scan and up to five data-dependent MS/MS scan (full MS/ddMS2). The five ions with the most intense signal detected in the full MS experiment scan (intensity threshold, 1.0×10^5) triggered a specific MS/MS spectrum. An exclusion list allowing to achieve the lowest limit of identification (LOI) was built from raw files containing solely the mobile phase. Full MS settings were as follows: resolution, 70,000 FWHM; scan range, *m/z* 125–650; automatic gain control (AGC) target, 1.0×10^6; and maximum injection time (MIT), 10 ms. ddMS2 settings were as follows: resolution, 17,500 FWHM; AGC target, 1.0×10^5; MIT, 100 ms; isolation mass window, 1 *m/z*, normalized collision energy (NCE), 55%; dynamic exclusion time, 9 s. The mass spectrometer was daily calibrated over a mass range 50–2000 *m/z*. Data were acquired with Xcalibur software (v.4.0, Thermo, Waltham, USA).

2.4.3 | Data processing and metabolites' rates calculation

Raw data were processed with the Compound Discoverer 3.1 software (Thermo, Waltham, USA), and metabolic profiles were generated using ChemDraw 15.0 software (PerkinElmer, Waltham, USA).

TABLE 1 Proposed O-PCE metabolites, names, biotransformation, exact mass, formula and two major fragments per compound with their related *m/z* and formula

ID	Name[a]	Bio- transformation	Exact mass		Major fragments	
			m/z	Formula	*m/z*	Formula
O-PCE	*N*-(2-oxo-1phenyl-cyclohex-1-yl)ethylamine or 2-(ethylamino)-2-phenylcyclohexanone = deschloro-*N*-ethyl-ketamine	N/A	218.15379	$^{C}_{14}H_{19}NO$	200.14359	$C_{14}H_{18}N$
					173.09619	$C_{12}H_{13}O$
M1	Biphenyle	Dehydration	155.08543	$^{C}_{12}H_{10}$	129.06976	$C_{12}H_{13}O$
					115.05436	C_9H_7
M2	1-Phenylcyclohexa-2,4(or 5)-dien-1-ol or 1,1′-biphenyl-1(2(or 4)*H*)-ol	Oxidative deamination	173.09596	$^{C}_{12}H_{12}O$	155.08556	$C_{12}H_{11}$
					145.10112	$C_{11}H_{13}$
M3	1-Phenyl-cyclohex-2-en-1-ol or 3,4-dihydro-[1,1′-biphenyl]-1(2*H*)-ol	Oxidative deamination	175.11182	$^{C}_{12}H_{14}O$	157.1010	$C_{12}H_{13}$
		Dehydration			131.08539	$C_{10}H_{11}$
M4 (O-PCA)	2-Oxo-1-phenyl-cyclohexylamine or 2-amino-2-phenyl-cyclohexanone = deschloro-norketamine	*N*-dealkylation	190.12227	$C_{12}H_{15}NO$	173.09612	$C_{12}H_{13}O$
					145.10106	$C_{11}H_{13}$
M5 (OH-PCA)	2-Hydroxy-1-phenyl-cyclohexylamine or 2-amino-2-phenyl-cyclohexan-1-ol = dihydro-deschloro-norketamine	*N*-dealkylation	192.13785	$C_{12}H_{17}NO$	119.04886	C_8H_7O
					91.05398	C_7H_7
M6 (DDH-PCE)	*N*-ethyl-[1,1′-biphenyl]-1(2*H*)-amine = didehydro PCE	Reduction	200.14334	$^{C}_{14}H_{17}N$	171.10439	$C_{12}H_{13}N$
		Dehydration			158.09654	$C_{11}H_{12}N$
M7 (OH-O-PCA)	2-Amino-2-(4(or 2,3)-hydroxyphenyl)cyclohexanone = 2, 3 or 4-phenol deschloro-norketamine or 2-amino-6(or 3, 4, 5)-hydroxy-2-phenyl cyclohexanone = 3, 4, 5 or 6-hydroxy deschloro-norketamine	Oxidation	206.1763	$^{C}_{12}H_{15}NO_2$	173.09634	$C_{12}H_{13}O$
					145.10110	$C_{11}H_{13}$
M8 (DH-O-PCE)	1-(Ethylamino)-5,6-dihydro-[1,1′-biphenyl]-2(1*H*)-one = dehydro O-PCE	Dehydration	216.13820	$C_{14}H_{17}NO$	171.08034	$C_{12}H_{11}O$
					143.08553	$C_{11}H_{11}$
M9 (OH-PCE)	*N*-(2-hydroxy-1-phenyl-cyclohex-1-yl)-ethylamine = hydroxy-PCE	Reduction	220.16939	$C_{14}H_{21}NO$	175.11153	$C_{12}H_{15}O$
					157.10094	$C_{12}H_{13}$
M10 (OH-DH-O-PCE)	1-(Ethylamino)-5-hydroxy-5,6-dihydro-[1,1′-biphenyl]-2(1*H*)-one = 5-hydroxy-dehydro O-PCE	Oxidation	232.13313	$^{C}_{14}H_{17}NO_2$	173.09616	$C_{12}H_{13}O$
					145.10117	$C_{11}H_{13}$
M11 (OH-O-PCE)	2-(Ethylamino)-2-(4(or 2,3)-hydroxyphenyl)cyclohexanone = 2, 3 or 4-phenol O-PCE or 2-(ethylamino)-6(or 3, 4, 5)-hydroxy-2-phenylcyclohexanone = 3, 4, 5 or 6-hydroxy O-PCE	Oxidation	234.14874	$^{C}_{14}H_{19}NO_2$	171.08041	$C_{12}H_{11}O$
					161.0959	$C_{11}H_{13}O$
M12 (DIOH-PCE)	2-(Ethylamino)-2-(4(or 2,3)-hydroxyphenyl)cyclohexan-1-ol = 2, 3 or 4 phenol-hydroxy-PCE or 2-(ethylamino)-6(or 3, 4, 5)-hydroxy-2-phenylcyclohexan-1-ol = 3, 4, 5 or 6 dihydroxy-PCE	Oxidation	236.16440	$^{C}_{14}H_{21}NO_2$	173.09607	$C_{12}H_{13}O$
					145.10123	$C_{11}H_{13}$
M13 (2-en-PCA-*N*-Glu)	1-Phenyl-cyclohex-2-enamine-*N*-glucuronide or 3,4-dihydro-[1,1′-biphenyl]-1(2*H*)-à-*N*-glucuronide	Dehydration	350.15924	$^{C}_{18}H_{23}NO_6$	122.09637	$C_8H_{12}N$
		N-glucuronidation			108.08064	$C_7H_{10}N$

TABLE 1 (Continued)

ID	Name[a]	Bio- transformation	Exact mass		Major fragments	
			m/z	Formula	*m/z*	Formula
M14 (O-PCA-*N*-Glu)	2-Oxo-1-phenyl-cyclohexanamine-*N*-glucuronide = deschloro-norketamine-*N*-glucuronide	*N*-glucuronidation	366.15408	$C_{18}H_{23}NO_7$	136.07561	$C_8H_{10}NO$
					119.04902	C_8H_7O
M15 (OH-O-PCA-O-Glu)	2-Amino-2-(4(or 2,3)-hydroxyphenyl)cyclohexanone-O-glucuronide = 2, 3 or 4-phenol deschloro-norketamine-O-glucuronide or 2-amino-6(or 3, 4, 5)-hydroxy-2-phenyl cyclohexanone-O-glucuronide = 3, 4, 5 or 6-hydroxy deschloro-norketamine-O-glucuronide	O-glucuronidation	382.14951	$C_{18}H_{23}NO_7$	188.10728	$C_{12}H_{14}NO$
					160.11203	$C_{11}H_{14}N$

Note: Metabolites were tagged with lowercase letters and sorted in ascending order of *m/z*.
Abbreviations: HLM, human liver microsomes; N/A, not applicable; ND, not detected; Rt, retention time.
[a]Names were given according to the most favoured structure of each compound.

Fragmentation patterns of O-PCE were studied taking into consideration those of ketamine and methoxetamine.[9,10,19]

The identification of compounds was performed by a specific metabolic workflow including phase I (e.g., oxidation, reduction and hydrolysis) and phase II (e.g., glucuronide conjugation and sulfatation) reactions. After uploading O-PCE chemical structure (in mol file format), raw data of HLMs incubate was processed after background subtraction. A prediction of potential metabolites, transformation pathways and corresponding structures were given according to exact mass, elemental composition, isotopic pattern and ddMS2 spectra.

In HLMs, metabolite rates (%) were expressed as the ratio of peak area of a metabolite to total peak area of all metabolites, excluding O-PCE peak area (corresponding to the remaining fraction after 2-h incubation). However, in biological samples (urine, hair), O-PCE peak area whenever present was considered in the calculation of total peak area as it represented the fraction of unchanged O-PCE excreted in urine or as a parent drug integrated into the hair shaft (Table 1).

2.4.4 | Application to authentic samples

Urine and hair samples were taken simultaneously along with a sample of crystalline solid labelled as O-PCE from a known O-PCE user (43 years old, male) after giving informed consent during harm reduction session, few days after his last O-PCE intake (by snorting). Due to this long delay, urine and hair were sampled; the latter was most likely to reveal O-PCE exposure as it offers a wide detection window. Two segments of hair A (proximal, 0–2 cm) and B (2–4 cm) reflecting an average exposure period of 4 months based on hair growth of 1 cm/month[20] were analysed. Crystalline solid was also recovered and analysed by the procedure described above. Raw data generated by LC-HRMS were processed by the metabolic workflow to cross-check the metabolites previously identified in HLMs incubates. Free urine and hair samples were analysed and processed simultaneously to subtract background signal. Validated metabolites from HLMs and authentic samples were included into the final metabolic pathway scheme.

3 | RESULTS AND DISCUSSION

3.1 | Identification of deschloro-*N*-ethyl-ketamine (O-PCE) by NMR

Data of 1H, 13C and 2D NMR (COSY, HSQC and HMBC) formally confirmed the structure of 2-(ethylamino)-2-phenylcyclohexanone (C14H19NO), known as deschloro-*N*-ethyl-ketamine or O-PCE. The product was pure at 99%. The carbon detected at 207.17 ppm (a) confirmed the presence of the ketone function in the aliphatic cycle. The carbon in the position 5 was characteristic of an alpha carbon of an amine. 1H NMR and 13C NMR spectra of O-PCE are presented in Figure S1a,b.

3.2 | O-PCE ddMS2 fragmentation

O-PCE was eluted at 6.5 min ([MH^+], *m/z* 218.15379) and was fragmented by neutral loss of water (*m/z* 200.14359) or ethylamine group (*m/z* 173.09596) followed by secondary neutral losses: dehydration (*m/z* 155.08543), carbon monoxide (*m/z* 145.10118), ethanone (*m/z* 129.06985), propanone (*m/z* 117.06985), butanone (*m/z* 105.0696) and pentanone (*m/z* 91.05421). Further fragmentations involved a cleavage between the benzene and the cyclohexanone ring leading to a loss of *N*-ethyl-2-oxo-cyclohexylamine (*m/z* 79.05441) group, or by a cleavage of the benzene ring generating *N*-ethyl-1-methyl-2-oxo-cyclohexylamine group (*m/z* 67.05437). O-PCE ddMS2 spectrum and assigned fragmentation patterns are given in Figure 2.

3.3 | O-PCE metabolites in HLMs

After 2 h incubation with HLMs, 15 metabolites were identified (M1 to M15), counting for 17% of total peak area (TPA), 83% being that of unchanged O-PCE that did not undergo biotransformation. For eight metabolites (M2, M3, M5, M9, M10, M11, M12 and M13), we identified a total of 18 features with the same exact mass and different retention indices that corresponded to potential isomers.

Two major metabolites were detected in HLMs: 1-phenylcyclohexa-2,4(or 5)-dien-1-ol (M2 with its two isomers) and deschloro-norketamine (M4, O-PCA), representing 86% of TPA of metabolites.

Table 1 gives a list of O-PCE and its potential metabolites, with proposed names, biotransformation pattern, exact mass, formula and major fragments (two for each compound).

Table 2 summarizes the peak area and the rates (%) of O-PCE and its detected metabolites in different analysed matrices (HLMs, urine, hair) with their corresponding retention times.

Metabolites (M1-M15) and their isomers (tagged with lowercase letters) are sorted in ascending order of *m/z* and retention times, respectively.

A proposed metabolic pathway combining all metabolites of O-PCE identified in HLMs and authentic samples are presented in Figure 3. Since NMR spectra were not available for the detected metabolites, some structure assignments are tentative, based on MS fragmentation.

The ddMS2 experiments yielded spectra that are reported in Figure S2.

Extracted ion chromatograms of O-PCE and its related metabolites are given in Figure S3.

O-PCE phase I metabolism involved three main metabolic pathways: *N*-dealkylation, oxidation and reduction. Phase II metabolism reactions were characterized by *O*- or *N*-glucuronidation of *N*-dealkylated or hydroxylated metabolites (M4, M5 and M7).

Overall, O-PCE metabolism seemed similar to that of methoxetamine, as described by Menzies et al.[10]

1. Oxidation

The oxidation of O-PCE and of its *N*-dealkylated metabolite O-PCA (M4) led to the hydroxylated derivative OH-O-PCE (M11) and its *N*-dealkylated analogue OH-O-PCA (M7), respectively. These two minor metabolites counted for less than 1% TPA. A further oxidation step occurred by the oxidation of DH-O-PCE (M8) to OH-DH-O-PCE (M10) where only one diastereomer (b) was detected in HLMs (0.8%).

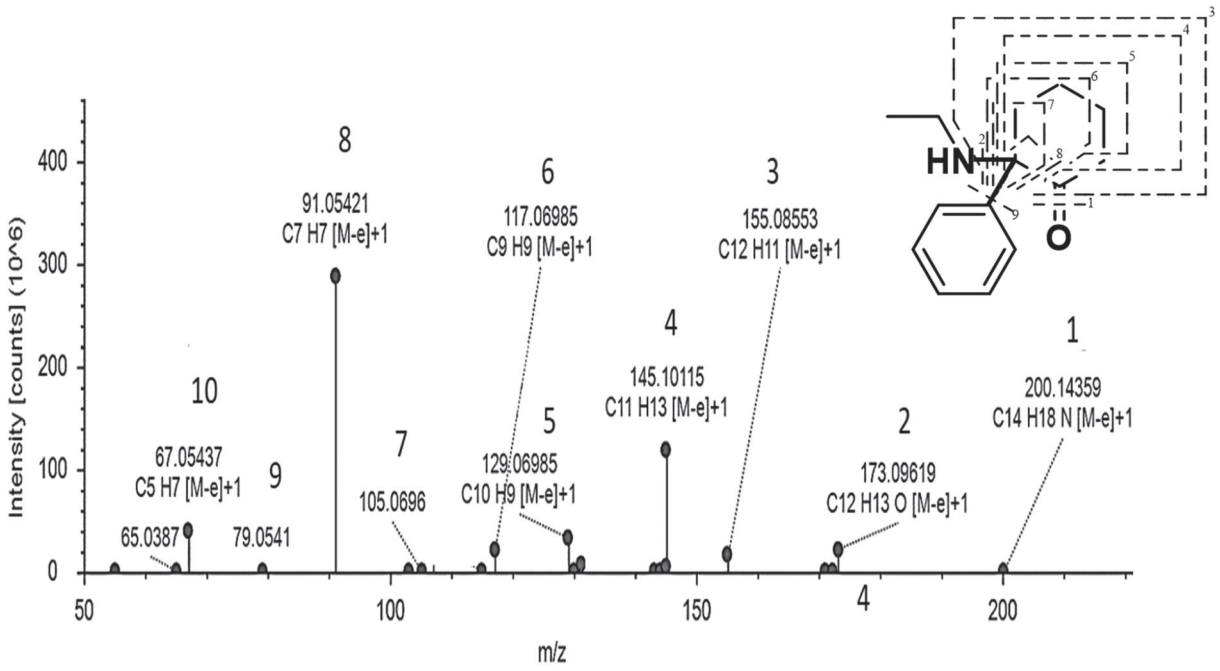

FIGURE 2 O-PCE ddMS2 spectrum with assigned fragmentation patterns

TABLE 2 Proposed O-PCE metabolites, names, exact mass, peak areas in HLMs, urine and hair samples and retention times

	Exact mass		Peak areas (counts)								
ID	*m/z*	Isomers	HLM	%[a]	Urine	%	Hair segment A (0–2 cm)	%[b]	Hair segment B (2–4 cm)	%[b]	Rt (min)
O-PCE	218.15379	NA	1.066E+10	83	ND	N/A	3.863E+07	12	4.355E+07	12.5	6.50
M1	155.08543	NA	1.222E+08	5	ND	N/A	2.952E+05	0.1	3.527E+05	0.1	6.50
M2	173.09596	a	2.619E+08	12	ND	N/A	ND	N/A	1.259E+06	0.5	5.79
		b	1.241E+09	55	ND	N/A	2.636E+06	0.8	3.047E+06	1	6.50
M3	175.11182	a	1.900E+06	0.1	2.502E+07	16	4.747E+06	1.5	6.172E+06	1.8	5.61
		b	4.655E+06	0.2	ND	N/A	1.178E+06	0.4	1.372E+06	0.4	7.06
M4 (O-PCA)	190.12227	NA	4.211E+08	19	5.371E+05	0.3	1.765E+06	0.5	1.724E+06	0.5	5.79
M5 (OH-PCA)	192.13785	a	ND	N/A	ND	N/A	2.405E+08	74	2.539E+08	73	11.67
		b	ND	N/A	ND	N/A	1.27E+07	3.9	1.76E+07	5	12.18
M6 (DDH-PCE)	200.14334	NA	8.371E+07	4	ND	N/A	ND	N/A	ND	N/A	6.50
M7 (OH-O-PCA)	206.1763	NA	3.010E+06	0.1	5.935E+05	0.4	ND	N/A	ND	N/A	6.96
M8 (DH-O-PCE)	216.13820	NA	3.652E+06	0.2	ND	N/A	1.403E+06	0.4	1.498E+06	0.4	6.04
M9 (OH-PCE)	220.16939	a	2.256E+07	1	4.549E+06	2.9	7.384E+06	2.3	6.651E+06	1.9	7.06
		b	1.775E+07	0.8	1.424E+07	9	8.388E+06	2.6	8.852E+06	2.6	7.46
M10 (OH-DH-O-PCE)	232.13313	a	ND	N/A	4.596E+06	2.9	ND	N/A	ND	N/A	2.95
		b	1.793E+07	0.8	ND	N/A	ND	N/A	ND	N/A	9.54
M11 (OH-O-PCE)	234.14874	a	ND	ND	2.35E+07	15	ND	N/A	ND	N/A	2.12
		b	2.09E+06	0.1	ND	N/A	ND	N/A	ND	N/A	4.12
		c	3.24E+07	1.5	ND	N/A	ND	N/A	ND	N/A	5.22
M12 (DIOH-PCE)	236.16440	a	ND	ND	6.08E+06	4	1.70E+06	0.5	ND	N/A	5.82
		b	1.35E+06	0.1	ND	N/A	ND	N/A	ND	N/A	6.41
M13 (2-en-PCA-*N*-Glu)	350.15924	a	ND	N/A	2.110E+07	13.5	3.218E+06	1	1.062E+06	0.3	6.61
		b	ND	N/A	1.272E+07	8	ND	N/A	ND	N/A	7.42
		c	ND	N/A	1.986E+07	12.6	ND	N/A	ND	N/A	8.71
M14 (O-PCA-*N*-Glu)	366.15408	NA	ND	N/A	2.422E+07	15.4	ND	N/A	ND	N/A	7.85
M15 (OH-O-PCA-*O*-Glu)	382.14951	NA	2.156E+06	0.1	ND	N/A	ND	N/A	ND	N/A	8.53

Note: Metabolites were tagged with lowercase letters and sorted in ascending order of *m/z*.

Abbreviations: HLM, human liver microsome; N/A, not applicable; ND, not detected; Rt, retention time.

[a]Percentage of metabolites was expressed as the ratio of peak area of a metabolite to total peak area of all metabolites, excluding that of O-PCE (remaining after HLM incubation).

[b]O-PCE peak area in hair was included in the calculation of total peak area (=100%) as parent drug and metabolites integrate hair in the same way.

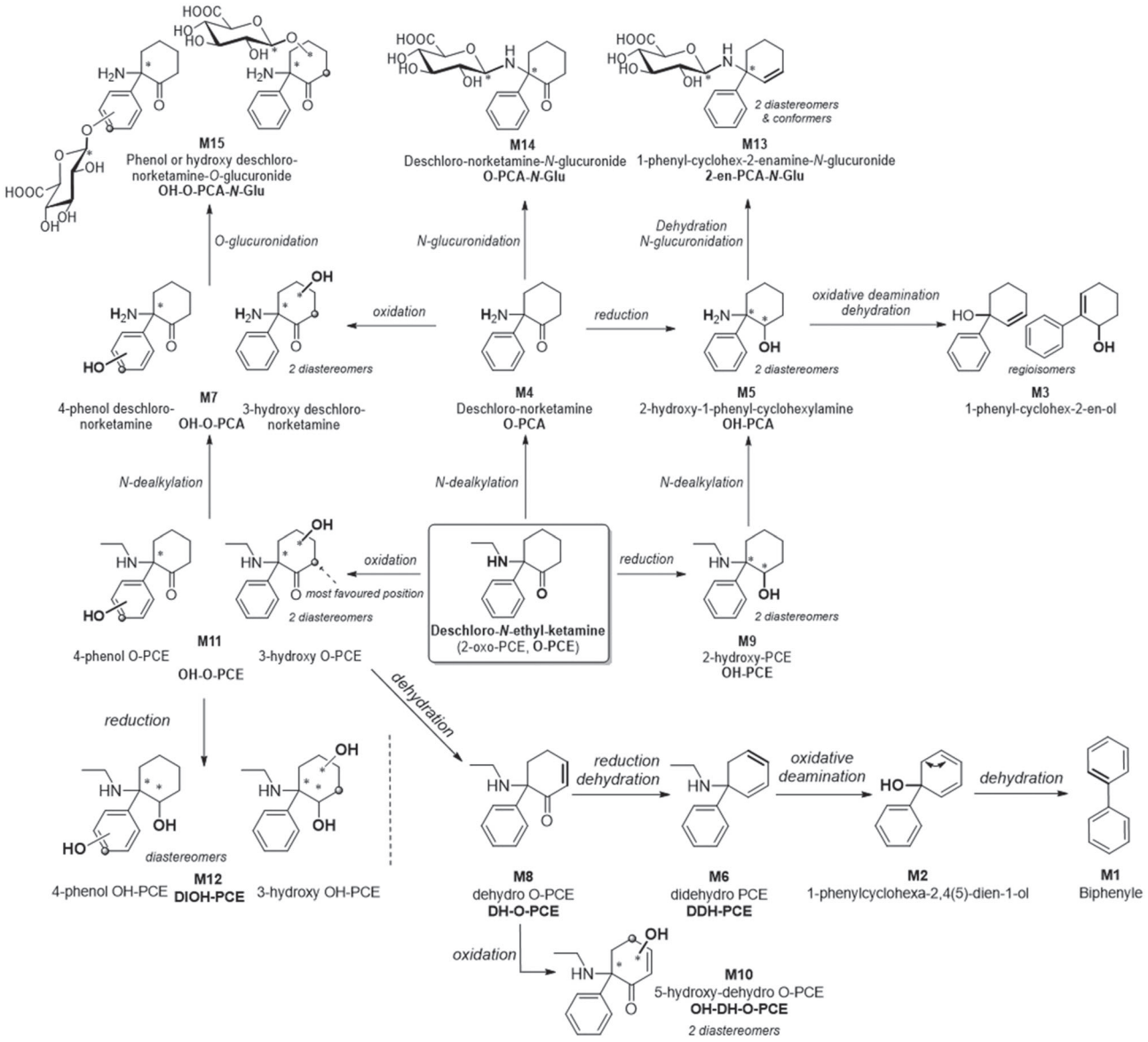

FIGURE 3 Proposed metabolic pathways of O-PCE in man

2. *N*-dealkylation

N-deethylation of O-PCE to the primary amine gave O-PCA (or deschloro-norketamine), which was the second most prevalent metabolite detected in HLMs, the first one being M2. O-PCA represented 19% of TPA and was the sole metabolite of O-PCE known so far.[5]

N-deethylation was also observed as a result of the biotransformation of M9 (OH-PCE) and M11 (OH-O-PCE) affording M5 (OH-PCA) and M7 (OH-O-PCA), respectively. OH-PCA was not detected in HLMs incubates, whereas OH-O-PCA was of minor relevance (<1% TPA).

3. Reduction

Different reactions involving the reduction of O-PCE or one of its metabolites were observed. Reduction of the carbonyl group of the O-PCE scaffold generated OH-PCE (M9). This reaction was characterised by a +2.0156 Da (+2H) shift observed from the parent drug. The mass difference was observed for the *m/z* fragments 173.09622, 155.0855, 131.0491 and 67.05437, but not for the *m/z* fragment 105.06959 (including the benzene moiety), which confirmed the reduction of the aliphatic part (Figure S2). Two chromatographic peaks (Rt 7.06 and 7.46 min) corresponding to the both generated diastereomers were detected, in accordance with the creation of two vicinal stereogenic carbon centres throughout the reduction of the racemic O-PCE. OH-PCE counted for up to 2% of TPA.

The reduction of the carbonyl function of O-PCA (M4) and OH-O-PCE (M11) generated, respectively, OH-PCA (M5) and DIOH-PCE (M12), with the identification of the corresponding diastereomers (M5 a/b, M12 a/b) as reported in Table 2. Only DIOH-PCE (M12 b) was detected in HLMs at low rate (<1%).

Reduction pathways were similar to those of methoxetamine[10] and represented about 11% of metabolites signal in HLMs.

4. Miscellaneous transformations including oxidative deamination and dehydration of reduced metabolites

Several metabolic transformations involved a dehydration step of the cyclohexane part. In that respect, OH-O-PCE (M11) was first dehydrated into the enone DH-O-PCE (M8), which was converted in DDH-PCE (M6) through the successive ketone reduction and dehydration of the nonobserved resulting alcohol. The two dehydrated metabolites M8 and M6 counted for 0.2% and 4% TPA in HLMs, respectively.If oxidative deamination has not been reported so far for ketamine or MXE,[9,19] this reaction seemed among the most relevant O-PCE biotransformation observed in HLMs.

The most relevant reaction corresponded to the oxidative deamination of DDH-PCE (M6) leading to the formation of M2 identified as two regioisomers (M2 a/b) according to the position of the second double bound at the C4 or the C5carbon of the cyclohexadienol moiety. M2 accounted for 67% of TPA in HLMs, where M2b was the most abundant (55% TPA). Finally, the dehydration of M2 gave the biphenyl (M1), which represents 5% of TPA.

Similarly, successive transformation steps of OH-PCA (M5) through an oxidative deamination and a consecutive dehydration of the resulting diol led to the formation of the enol M3 identified as two possible regioisomers according to the position of the phenyl ring at C1 (M3a) and C2 (M3b). This biotransformation pathway of OH-O-PCA was of minor relevance in HLMs (0.3% TPA).

5. Glucuronidation

Among the three identified *N*- and *O*-glucuronides (M13, M14 and M15), only the OH-O-PCA-*O*-glucuronide (M15) arising from the *O*-glucuronidation of M7 (OH-O-PCA) was detected in HLMs. According to the hydroxyl function position, on the aromatic (4-*phenol*-) or alicyclic (6-*hydroxy*-) ring, several stereoisomeric and regioisomeric *O*-glucuronides could be expected. However, only one matching peak was detected on the chromatogram. Moreover, this minor metabolite (0.1%) was not detected in human samples, probably due to a short elimination half-life and/or the late urine sampling. Another explanation could be the subcellular localization of UDP-glucuronlytransferases enzymes (UGT) in the internal membrane of the endoplasmic reticulum, limiting in vivo the access of substrates. This phenomenon known as 'latency' contributes to difficulties in extrapolating in vivo effects of UGT enzymes from in vitro experiments using isolated microsomes tissues.[21]

3.4 | O-PCE metabolic profile in urine and hair samples

Among the 12 metabolites identified in HLMs, 10 were detected in urine or hair. Three further metabolites (M5, M13, M14) were identified in urine and/or hair while absent from HLMs incubates (Table 2).

In urine, nine metabolites were identified, whereas O-PCE was no longer detected. The most relevant phase I metabolite was M3 (16%), followed by OH-O-PCE (15%) and OH-PCE (11.9%).

2-en-PCA-*N*-Glu with its related isomers (M13a/b/c) obtained as a result of OH-PCA glucuronidation was the most abundant metabolite excreted in urine (34% TPA). *N*-glucuronidation seems specific to O-PCE metabolism when compared with ketamine and MXE.[9,10,19] The absence of this glucuronide in HLMs incubates suggest that the glucuronidation occurred in extrahepatic tissues as some UGT isoforms were not present in the liver (e.g., UGT1A7, UGT1A8 and UGT1A10) and could explain why this glucuronide was missing in HLMs.[21]

Although O-PCA (deschloro-norketamine) was of minor relevance in urine (0.3%), its glucuronide (O-PCA-*N*-Glu) counted for 15.4% of TPA. Interestingly, the opposite finding has been observed in HLMs, where O-PCA was present (19%) but not its glucuronide. This could also be related to extrahepatic glucuronidation.

Therefore, in descending order of metabolite abundance, we suggest using 2-en-PCA-*N*-Glu (first), M3 (second), O-PCA-*N*-Glu (third), OH-O-PCE (fourth) and OH-PCE (fifth) as target metabolites to increase the detection window of O-PCE in urine.

In hair, O-PCE and nine metabolites were identified in both segments (except M2a detected only in segment B). OH-PCA (Log $P_{OH\text{-}PCA}$ = 1.55) was the most abundant metabolite accounting for 78% of TPA, while O-PCA was of minor relevance (0.5%) probably due to its high hydrophilicity (Log $P_{O\text{-}PCA}$ = 1.38) and poor integration into hair. In comparison with ketamine, it is well known that *N*-demethylation and dehydrogenation of ketamine (K) to the respective metabolites norketamine (NK) and dehydronorketamine (DHNK) are the major metabolic pathways. However, norketamine was the major metabolite in hair as reported by Favretto et al., whereas the presence of DHNK was excluded.[22] Interestingly, deschloro-norketamine/O-PCE ratio found in our study (mean = 0.042, *n* = 2) was very similar to that of NK/K (mean = 0.041, *n* = 2) reported by Favretto et al. However, in our study OH-PCA was present at high level with an OH-PCA/O-PCE ratio of 6, showing its good integration into keratin, even though it is more hydrophilic than its parent drug (Log $P_{OH\text{-}PCA}$ = 1.55 versus Log $P_{O\text{-}PCE}$ = 2.24). It is known that metabolites are less likely to integrate into hair than parent drug due to their higher hydrophilicity, but with regard to our finding, other mechanisms of integration into the hair matrix should be considered in the future.[20] The absence of OH-PCA in urine could be the consequence of its transformation to M13 and M3 as they were of major relevance in urine (50% TPA).

4 | LIMITATION OF THE STUDY

Since time and amount of ingestion of O-PCE were unknown, the results of urine analysis do not reflect the general excretion profile of O-PCE in human. Another limitation was the number of authentic sample (*n* = 1) used to validate the results of in vitro study. Consequently, further data are needed to confirm our findings.

5 | CONCLUSION

The present study showed an extensive metabolic profile of O-PCE in HLMs and authentic samples similar to that of methoxetamine and ketamine. Whereas M2 seemed presumably the most abundant metabolite in HLMs, 2-en-PCA-*N*-Glu (first), M3 (second), O-PCA-*N*-Glu (third), OH-O-PCE (fourth) and OH-PCE (fifth) were the most abundant metabolites in urine and were detected even when O-PCE was no longer excreted. Therefore, we recommend using these metabolites as target markers to increase the detection window of O-PCE in urine.

Even if it has been estimated to take approximately 7–10 days for the growing hair to reach the surface of the scalp,[20] which implies a detection gap (blind time) between urine and hair collection, hair appears to be a good alternative in drug metabolism study as an exploratory matrix, especially when urine collection is taken late after presumed consumption or was not sampled. It appears from our study that OH-PCA is of great interest for long-term monitoring of O-PCE exposure, as it integrates well into hair and had a relevant metabolite to parent drug ratio.

ORCID

Islam Amine Larabi https://orcid.org/0000-0002-9015-5342
Alice Ameline https://orcid.org/0000-0002-1117-0887
Pascal Kintz https://orcid.org/0000-0002-4174-5362

REFERENCES

1. World Drug Report 2019. https://wdr.unodc.org/wdr2019/prelaunch/WDR19_Booklet_5_CANNABIS_HALLUCINOGENS.pdf. Accessed September 29, 2020
2. Larabi IA, Fabresse N, Etting I. Prevalence of new psychoactive substances (NPS) and conventional drugs of abuse (DOA) in high risk populations from Paris (France) and its suburbs. *Drug Alcohol Depend*. 2019;204:107508. https://doi.org/10.1016/j.drugalcdep.2019.06.011
3. Stevens CL. Aminoketones and methods for their production. 1966. http://www.freepatentsonline.com/3254124.pdf. Accessed May 12, 2020.
4. Domino EF. Taming the ketamine tiger. *Anesthesiology*. 2010;113(3):678-684.
5. Cheng WC, Dao KL. The emergence of deschloro-*N*-ethyl-ketamine, a ketamine analog, in drug seizures and drug driving cases in Hong Kong. *J Anal Toxicol*. 2020;44(8):886-895. https://doi.org/10.1093/jat/bkaa038, https://doi.org/10.1093/jat/bkaa038
6. Tang MHY, Chong YK, Chan CY, et al. Cluster of acute poisonings associated with an emerging ketamine analogue, 2-oxo-PCE. *Forensic Sci Int*. 2018;290:238-243.
7. Theofel N, Möller P, Vejmelka E, et al. A fatal case involving N-Ethyldeschloroketamine (2-Oxo-PCE) and venlafaxine. *J Anal Toxicol*. 2019;43(2):e2-e6. https://doi.org/10.1093/jat/bky063, https://doi.org/10.1093/jat/bky063
8. Peters FT, Meyer MR. In vitro approaches to studying the metabolism of new psychoactive compounds. *Drug Test Anal*. 2011;3(7-8):483-495.
9. Meyer MR, Bach M, Welter J, Bovens M, Turcant A, Maurer HH. Ketamine-derived designer drug methoxetamine: metabolism including isoenzyme kinetics and toxicological detectability using GC-MS and LC-(HR-)MSn. *Anal Bioanal Chem*. 2013;405(19):6307-6321.
10. Menzies EL, Hudson SC, Dargan PI, Parkin MC, Wood DM, Kicman AT. Characterizing metabolites and potential metabolic pathways for the novel psychoactive substance methoxetamine. *Drug Test Analyst*. 2014;6:506-515.
11. Michely JAA, Manier SK, Caspar AT, Brandt SD, Wallach J, Maurer HH. New psychoactive substances 3-methoxyphencyclidine (3-MeO-PCP) and 3-methoxyrolicyclidine (3-MeO-PCPy): metabolic fate elucidated with rat urine and human liver preparations and their detectability in urine by GC-MS, "LC-(high resolution)-MSn" and "LC-(high resolution)-MS/MS". *Curr Neuropharmacol*. 2017;15(5):692-712.
12. Carlier J, Diao X, Scheidweiler KB, Huestis MA. Distinguishing intake of new synthetic cannabinoids ADB-PINACA and 5F-ADB-PINACA with human hepatocyte metabolites and high-resolution mass spectrometry. *Clin Chem*. 2017;63(5):1008-1021.
13. Kintz P, Richeval C, Jamey C, et al. Detection of the designer benzodiazepine metizolam in urine and preliminary data on its metabolism. *Drug Test Anal*. 2017;9(7):1026-1033.
14. Richeval C, Gicquel T, Hugbart C, et al. In vitro characterization of NPS metabolites produced by human liver microsomes and the HepaRG cell line using liquid chromatography high resolution mass spectrometry (LC-HRMS) analysis: application to furanyl fentanyl. *Curr Pharm Biotechnol*. 2017;18(10):806-814.
15. Ameline A, Richeval C, Gaulier JM, Raul JS, Kintz P. Detection of the designer benzodiazepine flunitrazolam in urine and preliminary data on its metabolism. *Drug Test Anal*. 2019;11(2):223-229.
16. Brum L. *Clinical Drug Interaction Studies—Cytochrome P450 Enzyme- and Transporter-Mediated Drug Interactions Guidance for Industry*. 2020. https://www.fda.gov/media/134581/download. Accessed September 29, 2020
17. Portalier F, Bourdreux F, Marrot J, Moreau X, Coeffard V, Greck C. Merging oxidative dearomatization and aminocatalysis: one-pot enantioselective synthesis of tricyclic architectures. *Org Lett*. 2013;15(22):5642-5645.
18. Fabresse N, Larabi IA, Stratton T, et al. Development of a sensitive untargeted LC-HRMS screening devoted to hair analysis through a shared MS2 spectra database: a step towards early detection of new psychoactive substances. *Drug Test Anal*. 2018;11:697-708.
19. Dinis-Oliveira RJ. Metabolism and metabolomics of ketamine: a toxicological approach. *Forensic Sci Res*. 2017;2(1):2-10.
20. Kintz P. *Hair Analysis in Clinical and Forensic Toxicology*. 1st ed. Boston, MA: Elsevier; 2015.
21. Raccor BS, Teitelbaum AM, Dinh J, Totah R. Principles of drug metabolism 3: enzymes and tissues, in: *Reference Module in Chemistry, Molecular Sciences and Chemical Engineering*, Elsevier, Oxford, 2014: pp. 167–191. https://doi.org/10.1016/B978-0-12-409547-2.11323-X
22. Favretto D, Vogliardi S, Stocchero G, et al. Determination of ketamine and norketamine in hair by micropulverized extraction and liquid chromatography–high resolution mass spectrometry. *Forensic Sci Int*. 2013;226(1-3):88-93.

SUPPORTING INFORMATION

Additional supporting information may be found online in the Supporting Information section at the end of this article.

How to cite this article: Larabi IA, Zerizer F, Ameline A, et al. Metabolic profiling of deschloro-*N*-ethyl-ketamine and identification of new target metabolites in urine and hair using human liver microsomes and high-resolution accurate mass spectrometry. *Drug Test Anal*. 2021;1–10. https://doi.org/10.1002/dta.3007